

Structural and Optoelectronic Properties of ZnSnO₃ Semiconductor

Mr. A. V. Patil^{a,*}, Dr S. B. Patil^b, Dr. P. V. Dalal^{c,*}

^{a,*}SSVPS late. Dr.P.R.Ghogrey Science College Deopur, Dhule- 424 002, Maharashtra, India

^bS. S. M. M. Arts, Science and Commerce College, Pachora- 424 201, Maharashtra, India

^{c,*}Nanomaterials Research Laboratory, Department of Physics, Shri. V. S. Naik, A.C.S. College, Raver, 425508, India

Abstract:

ZnSnO₃ is a promising ternary oxide semiconductor owing to its favorable structural, electrical, and optoelectronic properties. In this work, ZnSnO₃ samples were synthesized using a simple and cost-effective technique and characterized through thermoelectric power (TEP), electrical, and photosensing studies. Thermoelectric power measurements revealed a positive Seebeck coefficient, indicating p-type conductivity and dominant hole transport. Electrical studies showed temperature-dependent conductivity, confirming the semiconducting behavior of ZnSnO₃. Photosensing measurements under ultraviolet (UV) illumination demonstrated a significant enhancement in photocurrent compared to dark current, along with stable and repeatable photoresponse. The observed photosensing behavior is attributed to efficient generation of charge carriers and surface-related trapping mechanisms under light illumination. The combined results highlight the potential of ZnSnO₃ for applications in photodetectors and optoelectronic devices.

1. Introduction

Researchers are very interested in ternary oxide semiconductors because they can change their physical properties and can be used in many different ways in optoelectronics, sensing, and energy devices. Zinc stannate (ZnSnO₃) has become a promising material because of its unique electrical and structural properties. ZnSnO₃ usually crystallises in a structure linked to perovskite that is orthorhombic. By changing the conditions under which it is made, you can change its phase purity, crystallinity, and microstructure. Such structural

characteristics significantly affect its electrical and optical properties[1]. X-ray diffraction (XRD) is a typical way to study the structural properties of ZnSnO_3 . It shows that the phases are forming and the crystals are of good quality. XRD examinations of ZnSnO_3 nanoparticles frequently demonstrate an orthorhombic perovskite phase, signifying distinct lattice configurations that enhance effective charge transport. [1] Additionally, synthesis parameters like pH, precipitation conditions, and calcination temperature have a big effect on the size of the crystallites and the strain in the lattice, which in turn affects the optoelectronic performance[2].

ZnSnO_3 has a broad band gap in the near-UV region, which makes it great for detecting ultraviolet light and for use in clear electronic devices. Studies using UV-visible spectroscopy have found that the band gap values for ZnSnO_3 nanoparticles are between 3.5 and 3.7 eV, which is compatible with how wide-bandgap semiconductors work. This broad band gap lets UV light be absorbed well while keeping the visible spectrum clear, which is critical for optoelectronic devices like UV photodetectors and clear conductors[3]. The optoelectronic characteristics of ZnSnO_3 are intricately associated with its charge carrier dynamics and photodetection abilities. Photogenerated carriers improve electrical conductivity when exposed to UV light. This effect is used in photodetectors and photoresponsive sensors. Recent investigations show that ZnSnO_3 -based structures have a strong photoresponse, which is similar to other wide band gap oxide semiconductors. This shows that ZnSnO_3 could be useful for high-performance photosensing applications[4]. ZnSnO_3 is still being studied for use in sophisticated optoelectronic and sensing technologies because it has a stable structure, a large optical band gap, and reacts to light. Nonetheless, comprehending the interaction among crystal structure, defect densities, and carrier transport is essential for enhancing device performance[6-11].

2. Experimental details

2.1. Preparation of ZnO-SnO_2 nanocomposites and perovskite ZnSnO_3 thin films

Nanocomposite and perovskite thin films have been synthesized on glass substrates by employing spray pyrolysis technique. To create nanocomposite thin films of ZnO-SnO_2 and perovskite ZnSnO_3 on a glass substrate that has been preheated, zinc chloride (ZnCl_2 from Merck, extra pure) and tin (II) chloride pentahydrate ($\text{SnCl}_2 \cdot 5\text{H}_2\text{O}$ from Merck, extra pure)

were utilized. Table 1 shows the results of mixing zinc chloride with tin (II) chloride pentahydrate in various ratios, including 25:75, 50:50, and 75:25 (1:3, 1:1, and 3:1).

Table 1: Varying amount of reactants and spraying solutions

Thin film Sample	ZnCl ₂ (cm ³)	SnCl ₂ .5H ₂ O (cm ³)	Volume Ratio	Reactants
S1	25	75	1:3	ZnO-SnO ₂
S2	50	50	1:1	ZnO-SnO ₂
S3	75	25	3:1	ZnSnO ₃

Based on the composition, the prepared films were label as S1 and S2 (both nanocomposites ZnO-SnO₂), and S3 (perovskite based ZnSnO₃ thin films). Depending on the size of the droplets, the chemical reaction, droplet landing, and solvent evaporation all play a critical role in the creation of the film. We optimized the synthesis parameters are listed in Table 2. The carrier gas pressure, to and fro nozzle movement and substrate temperature were kept constant during the process. Notably, the point during which the droplet approaches the glass substrate sufficiently for the solvent to completely evaporate is the optimal condition for film creation. The synthesized nanocomposites ZnO-SnO₂ and perovskite ZnSnO₃ thin films samples were annealed at 500 °C for 1 h in the presence of air to enhance its electrical, morphological, microstructure properties and gas sensing capabilities.

3. Characterization of thin films:

3.1 Electrical properties:

A) TEP measurement

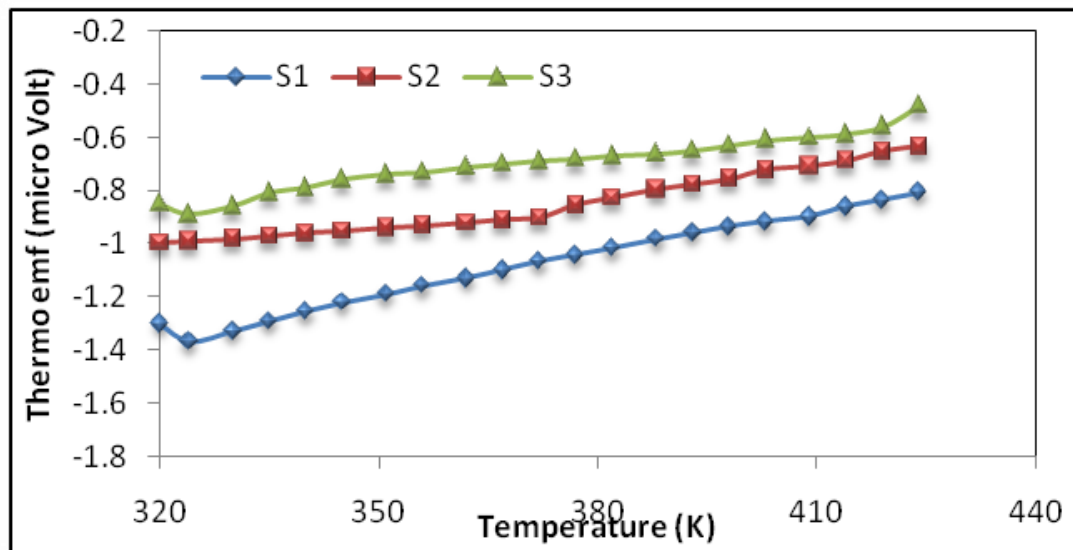


Figure 1: Temperature dependence of thermoelectric power measurement.

An Arrhenius plot of ZnO-SnO₂ and ZnSnO₃ thin films is shown in Fig. 2. Figure 3.5 shows temperature curves and thermoelectric power for thin films of ZnO-SnO₂ and ZnSnO₃ with different compositions (different amounts of Zn and Sn). Figure 2 clearly shows that the thermoelectric power of all samples goes up as the temperature goes up. TEP is negative for all samples in the temperature range of 320–424 K, indicating n-type conductivity [15,16]. All of the samples act like semiconductors. The difference in temperature in the thermoemf measurement makes a carrier migrate from the hot end to the cold end. This generates an electric field that calculates the thermal voltage. The difference in temperature across the semiconductor is exactly equal to this voltage that is created by heat. The thermoemf was positive at the hot end compared to the cold end, which showed that ZnO-SnO₂ and ZnSnO₃ films are n-type conductors.

B) Electrical conductivity

The electrical conductivity of the nanocrystalline thin films was measured using the DC two-probe method in the temperature range of 298–423 K. The conductivity (σ) was evaluated using the Arrhenius-type relation (1):

$$\sigma = \sigma_0 e^{\frac{-\Delta E}{kT}} \quad \text{-----} \quad (1)$$

where σ_0 is the pre-exponential factor, ΔE is the activation energy, k is the Boltzmann constant, and T is the absolute temperature.

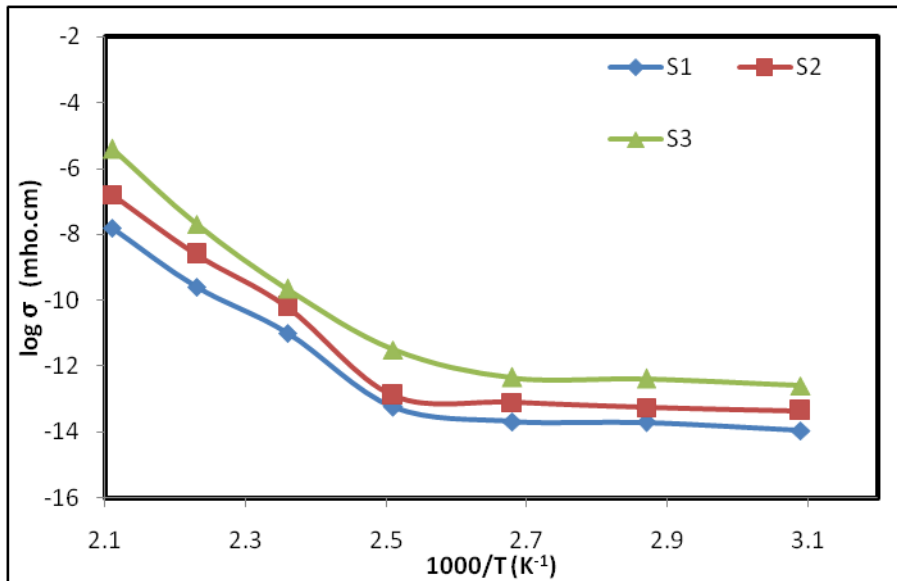


Figure2. Variation of $\log(\sigma)$ with inverse of operating temperature (K)

Figure 3 shows the variation of $\log(\sigma)$ with the inverse of temperature ($1000/T$). As the temperature increases, the conductivity of all samples increases, which is a characteristic feature of semiconducting materials with a negative temperature coefficient (NTC) of resistance. This confirms that the nanocrystalline thin films exhibit semiconducting behaviour [13].

The conductivity studies reveal two distinct activation energy regions, corresponding to low- and high-temperature ranges at 323-373 K and 373-423 K respectively. The activation energy values, extracted from the slopes of the $\ln(\sigma)$ versus $1/T$ plots, are summarized in Table 2. The presence of two activation energies indicates two donor levels - one deep and one shallow - located near the conduction band edge. At higher temperatures (423 K), the activation energy decreases slightly, which can be attributed to oxygen adsorption at the film surface. The adsorbed oxygen atoms capture free electrons from the conduction band and form weak bonds with zinc atoms, thereby affecting the conduction process through surface states.

Sample	Thickness (nm)	Activation energy (ΔE)	
		323 K (Low temperature)	423 K (High temperature)
S1	810	0.23 eV	0.19 eV
S2	843	0.17 eV	0.14 eV
S3	839	0.19 eV	0.17 eV

Table 2: Measurement of thickness with activation energy

It is evident from Table 2 that the activation energy decreases with increasing film thickness (S1 to S2). This behavior is likely due to improved crystallinity and grain growth with thickness, which reduces grain boundary scattering and enhances carrier mobility. However, for sample S3, although the thickness decreases slightly compared to S2, the activation energy increases. This anomalous behavior may be associated with structural modifications, possibly the formation of a perovskite-like phase, which alters the electronic structure and increases the barrier for conduction [14]. Thus, the combined analysis of conductivity behavior and activation energy trends highlights the role of microstructural features and surface states in governing the charge transport mechanism in the nanocrystalline thin films.

3.3. Photosensing of ZnO-SnO₂ and ZnSnO₃ sample:

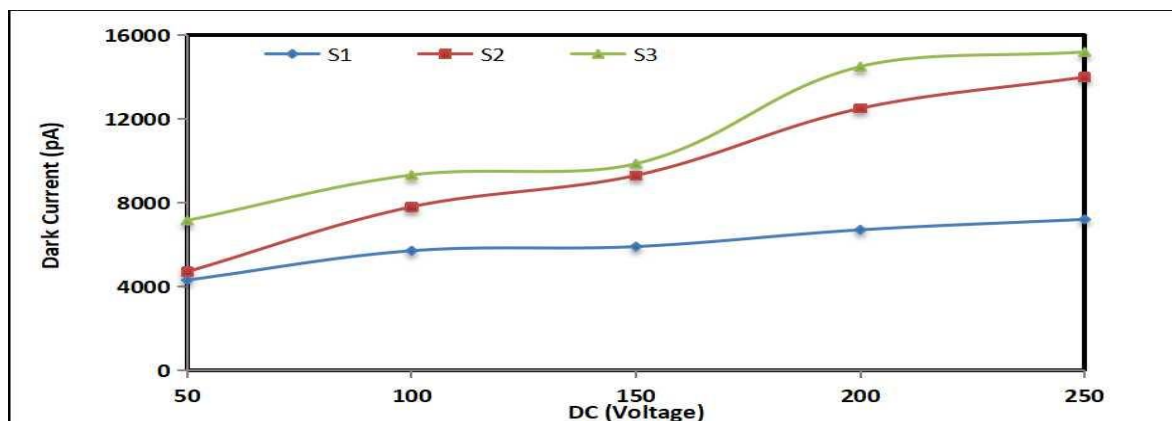


Figure 3. Dark current (pA) vs DC voltage (V) for three samples (S1, S2, S3).

Figure demonstrates how the dark current changes when different DC voltages are applied to samples S1, S2, and S3. For all samples, the dark current goes up steadily as the voltage goes up. This shows that the electrical conduction is stable and the electrode contact is good. S3 has the most dark current of the three samples, whereas S1 has the least current across the whole measured voltage range. The behaviour shown can be explained by differences in the concentration of charge carriers and the density of defects in the samples. The low dark current seen in sample S1 is very useful for photosensing applications because it improves the signal-to-noise ratio when there is light[16].

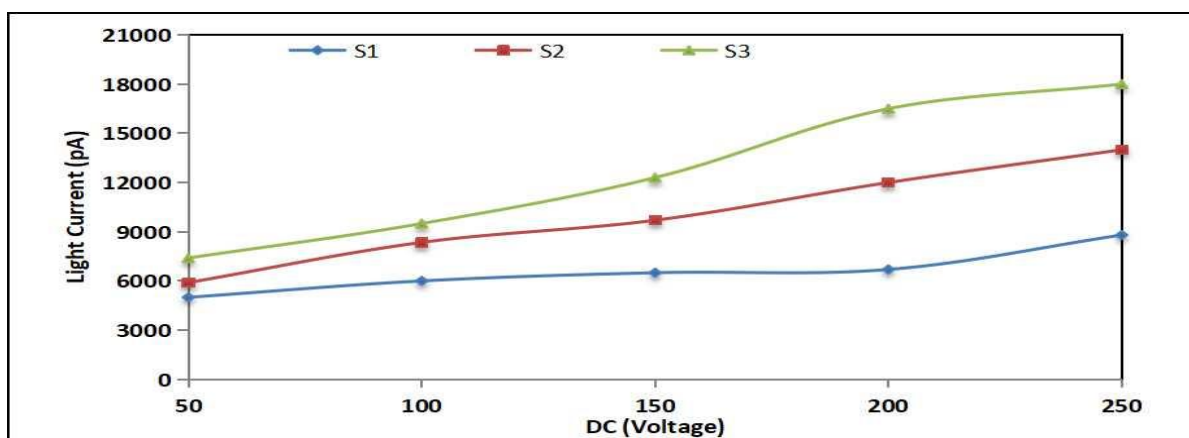


Figure5. Illumination current (pA) Vs DC voltage (V) for three samples (S1, S2, S3).

When light is shown on them, all of the samples show a clear increase in current when the DC voltage goes up, which shows that they are photosensitive. Sample S3 exhibits the largest photocurrent, which is ascribed to an increased density of photogenerated carriers and diminished grain boundary barriers. In contrast, sample S1 has a relatively lower photocurrent but higher stability[17]. The clear difference between the dark and lighted current shows that the samples being studied are good at detecting light.

Conclusion:

The research shows that thin films of ZnO-SnO₂ and ZnSnO₃ made by spray pyrolysis have good structural and morphological properties. The size of the crystals gets smaller as the Zn-to-Sn ratio changes. Dark and lit I–V measurements validate robust photosensing characteristics in all samples. Sample S3 has the largest photocurrent and

photosensitivity because it makes more photocarriers, while S1 has a low dark current that is good for low-noise detection.

Acknowledgement:

The authors thank Shri. V.S. Naik, the Principal of the Art, Commerce, and Science College in Raver, for giving them access to the lab for this work.

References:

1. *J Sol-Gel SciTechnol* **112**, 703–714 (2024). <https://doi.org/10.1007/s10971-024-06550-2>
2. <https://doi.org/10.3390/engproc2025087004>
3. <https://doi.org/10.1016/j.jallcom.2024.174854>
4. I. M. El Radaif Promising novel transparent conductive F-doped ZnSnO₃ thin films for optoelectronic applications, *J. Mater. Sci.: Mater. Electron.*, 2023,
5. <https://doi.org/10.1039/D3RA05481K>
6. N. Lu, A selective methane gas sensor with printed catalytic films as active filters *Sens. Actuat. B Chem* (2021)
7. T. Hübert, Hydrogen sensors – A review *Sens Actuators B Chem*, (2011)
8. L.N. Acquaroli et al. Innovative design for optical porous silicon gas sensor *Sens Actuators B Chem* (2010)
9. Y. Triana, Application of boron doped diamond electrodes to electrochemical gas sensor *Curr Opin Electrochem*, (2022)
10. Sagarika Panda, Savita Mehlaawat, Neeraj Dhariwal, Ashwani Kumar, Amit Sanger, *Materials Science and Engineering: B Volume 308*, (2024), 117616
11. Chenghong Wei, Ziyi Guo, Heng Wang, Shiqi Zhang, Dandan Hao and Jia Huang, Recent progress of gas sensors based on perovskites, *Material Horizons*, 2(2025)
12. U.R. Shwetha, M.S. Latha, C.R. Rajith Kumar, M.S. Kiran, V.S. Betageri, Facile synthesis of zinc oxide nanoparticles using novel Areca catechu leaves extract and their in

- vitro antidiabetic and anticancer studies, J. Inorg. Organomet. Polym. Mater. 30 (12) (2020) 4876–4883.
13. U.R. Shwetha, M.S. Latha, C.R. Rajith Kumar, M.S. Kiran, V.S. Betageri, Facile synthesis of zinc oxide nanoparticles using novel Areca catechu leaves extract and their in vitro antidiabetic and anticancer studies, J. Inorg. Organomet. Polym. Mater. 30 (12) (2020) 4876–4883.
14. S. Deepa, K. PrasannaKumari, B. Thomas, Contribution of oxygen-vacancy defect-types in enhanced CO₂ sensing of nanoparticulate Zn-doped SnO₂ flms. Ceram. Int. 43, 17128–17141 (2017). <https://doi.org/10.1016/j.ceramint.2017.09.134>
15. J. Wang, Z. Chen, Y. Liu, C.-H. Shek, C.M.L. Wu et al., Heterojunctions and optical properties of ZnO/SnO₂ nanocomposites adorned with quantum dots. Sol. Energy Mater. Sol. Cells 128, 254–259 (2014). <https://doi.org/10.1016/j.solmat.2014.05.038>
16. Author(s). (2024). High-performance solar-blind photodetectors based on Ta-doped ZnSnO₃ single crystal thin films, Journal of Alloys and Compounds, 997, 174854. <https://doi.org/10.1016/j.jallcom.2024.174854>
- C. Hu, L. Chen, Y. Hu, A. Chen, L. Chen et al., Light-motivated SnO₂/TiO₂ heterojunctions enabling the breakthrough in energy density for lithium-ion batteries. Adv. Mater. 33, e2103558 (2021). <https://doi.org/10.1002/adma.202103558>
17. Author(s). (2022). Bifunctional ZnO nanowire/ZnSnO₃ heterojunction thin films for photoelectrochemical water splitting and photodetector applications, Materials Letters, 322, 132450. <https://doi.org/10.1016/j.matlet.2022.132450>